Eur. Polym. J. Vol. 25, No. 11, pp. 1173–1182, 1989
Printed in Great Britain.

0014-3057/89 $3.00 + 0.00

A STATISTICAL MODEL FOR THE RANDOM PACKING OF REAL POWDER PARTICLES

D. J. CUMBERLAND,[1] R. J. CRAWFORD[1] and D. SPREVAK[2]

[1]Department of Mechanical and Manufacturing Engineering and [2]Department of Engineering Mathematics, Ashby Institute, Stranmillis Road, Belfast BT9 5AH, Northern Ireland
[*Tel.* 661111; *Telex* 74487]

(*Received* 31 *October* 1988)

Abstract—A statistical model for the packing of irregularly shaped powder particles has been developed. It has been based on experimental measurements for the packing of specially synthesized particle size distributions of poly(vinylidene chloride) powder. It is shown that, as the coefficient of variation (ratio of standard deviation/mean particle size) decreases, so does the fraction of theoretical density. It is also shown that for real powders the packing density is very low, with predicted values being only about one third of the values obtained in idealized random packing of spherical particles. The difference is attributed to the irregular shape of real particles and additional factors such as friction, adhesion and surface forces which are very sensitive to particle size.

INTRODUCTION

When powdered material is put into a container, the arrangement of the particles and the consequent distribution of voids between the particles has a major influence on the subsequent behaviour of the powder mass. The importance of this topic to the metallurgical, pharmaceutical and ceramic industries, for example, is reflected in the wide range of publications which have emerged in this field. They have been reviewed [1] and it is apparent that the complexity of the problem has made it necessary to introduce simple models in order to perform any type of mathematical analysis. Therefore most of the published work to date has concentrated on the packing of spherical particles. The starting point is mono-size spheres; this problem is straightforward but the complexity builds up as binary, ternary, quaternary, quinary and eventually n-component systems are considered.

This work has been valuable in presenting a picture of the densification of particulate systems but from the industrial point of view it has limited applicability. This is because there are additional unaccounted factors which affect the packing of real particles. For example, most real powders contain non-spherical particles. As a result of the irregularity of the particles, the packing densities which can be achieved are known to be considerably less than the theoretical predictions based on the assumption of spherical particles. It is not surprising that very little theoretical or experimental work has been done with real powders due to the complexity of the problem and the large permutations of variables.

In an attempt to shed some light on this problem, a simple model has been developed for the packing of real (irregular shaped) particles. This involves a statistical mathematical approach backed up by experimental measurements of the packing of powders having specially selected particle size distributions.

EXPERIMENTAL PROCEDURES

The powder chosen was "Viclan" poly(vinylidene chloride) (PVdC) Copolymer Resin VR562 (Fig. 1). A large quantity of this powder was vibrated through 12 Endecotts sieves using a sieve shaker (Pascall Engineering Co Ltd). The sieve aperture sizes are listed in Table 1 and Fig. 1. The small quantity of extremely fine particles of powder dust (0.08 g), which fell through the 53 μm aperture sieve into the receiver was discarded, as was the coarse particles of powder (30.02 g) remaining in the 1700 μm aperture sieve. The quantity of the powder that was retained (97.97%) was then conveniently divided into 11 discrete intervals, which together were representative of the particle size distribution for the PVdC powder. These intervals were numbered beginning with the small particle sizes. Figure 2 shows the sieve analysis of the PVdC powder drawn in histogram form on a logarithmic scale, together with the cumulative distribution. To take account of the differences in width of each interval, it is necessary to divide the relative frequency of particles in each interval by its interval width to obtain the relative frequency per unit interval. A histogram normalized in this way was then drawn as shown in Fig. 3. Several different theoretical distributions were superimposed on the data in this histogram and the goodness of fit was tested using the Kolmogorov–Smirnov Test [2]. This test showed that the lognormal distribution was best and is consistent with the data.

In Table 1 the mean particle size (μm) for each interval was calculated and the weight of particles in each interval established. This Table also shows the weight percentage of particles, the relative frequency, the sieved interval width and the relative frequency per unit interval for each interval. The second half of the Table gives probability calculations for the complete continuous distribution. Hence it is possible to calculate the following parameters of the mean or expectation and the SD.

The mean diameter of the particles is:

$$\mu = \sum_{x \in \Omega_x} x \cdot p_x(x) \tag{1}$$
$$= 221.98\ \mu\text{m}$$

and its variance:

$$\sigma^2 = \sum_{x \in \Omega_x} (x - \mu)^2 \cdot p_x(x) \tag{2}$$
$$= 11456.04$$

so the SD is

$$\sigma = \sqrt{11456.04} = 107.03\ \mu\text{m}. \tag{3}$$

Table 1. Results and probability calculations for the

Size band (μm) Lower–Upper	Interval No.	Mean particle size in interval x (μm)	Weight of particles in each interval w (g)	Weight % of particles $= W/\Sigma W \times 100$	Relative frequency f	Sieved interval width (μm) I
Receiver–53	—	—	—	—	—	—
53–75	1	64.0	0.35	0.024	0.0002	22
75–106	2	90.5	11.55	0.744	0.007	31
106–150	3	128.0	83.70	5.755	0.0575	44
150–212	4	181.0	700.02	48.129	0.4813	62
212–300	5	256.0	392.42	26.980	0.2698	88
300–355	6	327.5	88.23	6.066	0.0607	55
355–425	7	390.0	48.42	3.329	0.0.333	70
425–600	8	512.5	54.28	3.732	0.0373	175
600–850	9	725.0	37.40	2.571	0.0257	250
850–1180	10	1015.0	19.46	1.338	0.0134	330
1180–1700	11	1440.0	18.63	1.281	0.0128	520
1700–>1700	—	—	—	—	—	—
			$\Sigma = 1454.46$	$\Sigma = 100.00$	$\Sigma = 1.00$	

From the above it is now possible to calculate the ratio $v = \sigma/\mu$ called the population *coefficient of variation* or *coefficient of dispersion.*

$$\sigma/\mu = 107.03/221.98$$
$$= 0.482.$$

The two parameters of this ratio uniquely define this continuous distribution so the following statistical model for the random packing of real particles was developed.

STATISTICAL MODEL FOR THE RANDOM PACKING OF REAL PARTICLES

Let V = the total volume (volume occupied) of particles per unit volume (UV),
V_i = the volume of the ith particle per UV,
$v = V/N$ = the mean particle volume per UV,
N = the total number of particles per UV.

Hence:

$$V = V_1 + V_2 + V_3 + \cdots + V_i + \cdots + V_N. \quad (4)$$

Thus, the random variable V is the sum of N random variables V_i.

Taking expectations:

$$E(V) = E(N) \cdot \sum_{i=1}^{N} E(V_i/N).$$

The V_is have the same distribution, thus

$$E(V) = E(N) \cdot E(V/N) = E(N) \cdot E(v) \quad (5)$$

where $E(v)$ = the expected volume of a particle, per UV.
Then,

$$E(V) = c \cdot E(\mu^3) \cdot E(N) \quad (6)$$

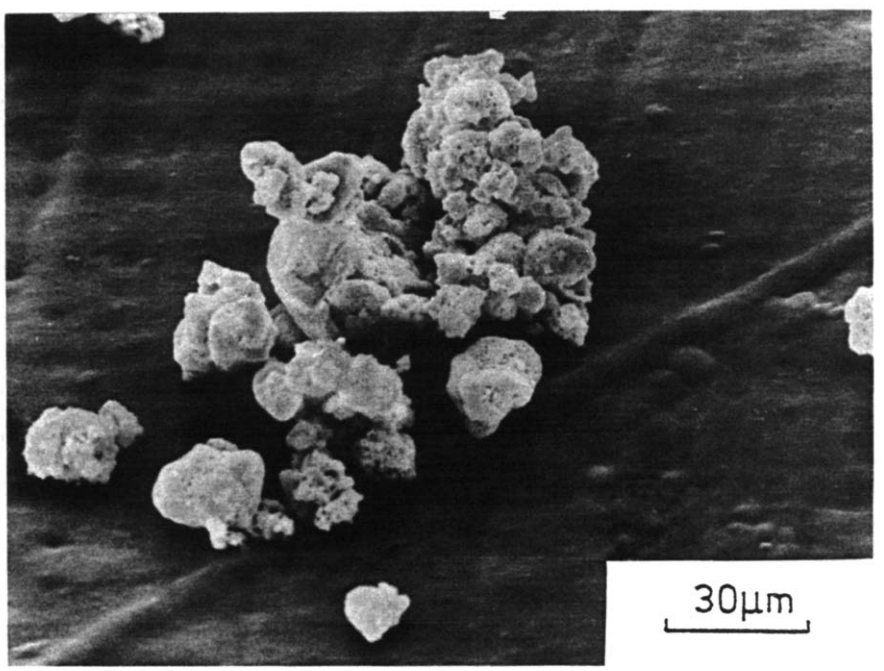

Fig. 1. Micrograph of PVdC powder.

complete continuous distribution of PVdC powder

Relative frequency per unit interval f/I	$\rho(x)=\frac{f/I}{\Sigma f/I}$	$x\cdot\rho(x)$	$x^2\cdot\rho(x)$	$x^3\cdot\rho(x)$	$x-\mu$	$(x-\mu)^2$	$\rho(x)(x-\mu)^2$
—	—	—	—	—	—	—	—
1.09E-5	0.0008	0.05	3.11	198.94	−157.98	24956.80	18.94
25.62E-5	0.0178	1.61	146.09	13220.96	−131.48	17286.25	308.33
130.79E-5	0.0911	11.66	1491.87	190959.35	−93.98	8831.71	804.19
776.28E-5	0.5404	97.82	17705.67	3204725.00	−40.98	1679.13	907.49
306.60E-5	0.2135	54.64	13989.07	3581197.40	34.02	1157.55	247.09
110.28E-5	0.0768	25.15	8235.61	2697159.50	105.51	11135.06	855.00
47.56E-5	0.0331	12.91	5036.26	1964141.10	168.02	28231.66	934.79
21.33E-5	0.0149	7.61	3900.45	1998973.40	290.52	84403.50	1253.39
10.29E-5	0.0072	5.19	3765.52	2730004.70	503.02	253031.94	1812.70
4.05E-5	0.0028	2.86	2904.82	2948399.30	793.02	628885.16	1773.20
2.46E-5	0.0017	2.47	3551.45	5114087.90	1218.02	1483579.50	2540.93
—	—	—	—	—	—	—	—
Σ = 1436.36E-5	Σ = 1.0	Σ = 221.98	Σ = 60729.91	Σ = 24443068			Σ = 11456.04

where c is a constant, the "shape factor", which depends on the assumed shape of the particles and μ is the mean particle diameter.

The mean number of particles per UV, $E(N)$, is some function of the ratio σ/μ. This choice of independent variable was selected in order to have a dimensionless variable which takes account of the size of μ and σ. Therefore:

$$E(N)=f_N(\sigma/\mu) \tag{7}$$

substituting equation (7) into (6) gives:

$$E(V)=c\cdot E(\mu^3)\cdot f_N(\sigma/\mu) \tag{8}$$

rearranging gives:

$$\frac{E(V)}{c\cdot E(\mu^3)}=\frac{E(V)}{E(v)}=f_N(\sigma/\mu). \tag{9}$$

Equation (9) shows that the ratio of the mean volume of all the particles per UV to the mean particle volume per UV is equal to some function of the ratio σ/μ.

To find the mean particle volume per UV, assume that all the particles are spherical.
Then

$$v=\frac{\pi}{6}\mu^3 \tag{10}$$

where μ is the diameter of the sphere of volume v.
Thus

$$E(v)=\frac{\pi}{6}\cdot E(\mu^3). \tag{11}$$

In order to estimate the mean number of particles per UV in equation (9), let:

Absolute solids density of powder

$$=\frac{\text{Total weight of spherical particles in volume occupied}}{\text{total volume occupied}}$$

$$\rho_a=\frac{\text{weight}}{\text{mean number of particles per } UV \times \text{the mean particle volume per } UV} \tag{12}$$

$$\rho_a=\frac{W}{f_N\cdot\frac{\pi}{6}E(\mu^3)}=\frac{6W}{\pi\cdot f_N\cdot E(\mu^3)}. \tag{13}$$

Transposing for f_N gives:

$$f_N=\frac{6W}{\pi\cdot\rho_a\cdot E(\mu^3)}. \tag{14}$$

To find the shape factor c, substitute equation (14) into (9):

$$\frac{E(V)}{c\cdot E(\mu^3)}=\frac{6W}{\pi\cdot\rho_a\cdot E(\mu^3)}$$

$$\frac{E(V)}{c}=\frac{6}{\pi}\cdot\frac{W}{\rho_a}$$

since $E(V)=W/\rho_a$, then

$$c=\pi/6.$$

Substituting this value into equation (9) yields:

$$\frac{6\cdot E(V)}{\pi\cdot E(\mu^3)}=f_N(\sigma/\mu)$$

$$E(V)=\frac{\pi}{6}\cdot E(\mu^3)\cdot f_N(\sigma/\mu). \tag{15}$$

The fraction of theoretical density (FTD) can then be written as:

$$FTD=\frac{\text{volume occupied}}{\text{total volume}}=\frac{W/\rho_a}{UV}$$

$$=\frac{\text{weight in } UV}{\text{total weight}}=\frac{W}{\rho_a\cdot UV} \tag{16}$$

$$=E(V)/UV$$

$$FTD=\frac{\pi}{6\cdot UV}\cdot E(\mu^3)\cdot f_N(\sigma/\mu). \tag{17}$$

Note that $E(\mu^3)\neq[E(\mu)]^3$ in equation (17). The 3rd moment of μ i.e. $E(\mu^3)$ for the complete continuous distribution can be obtained from the summation of

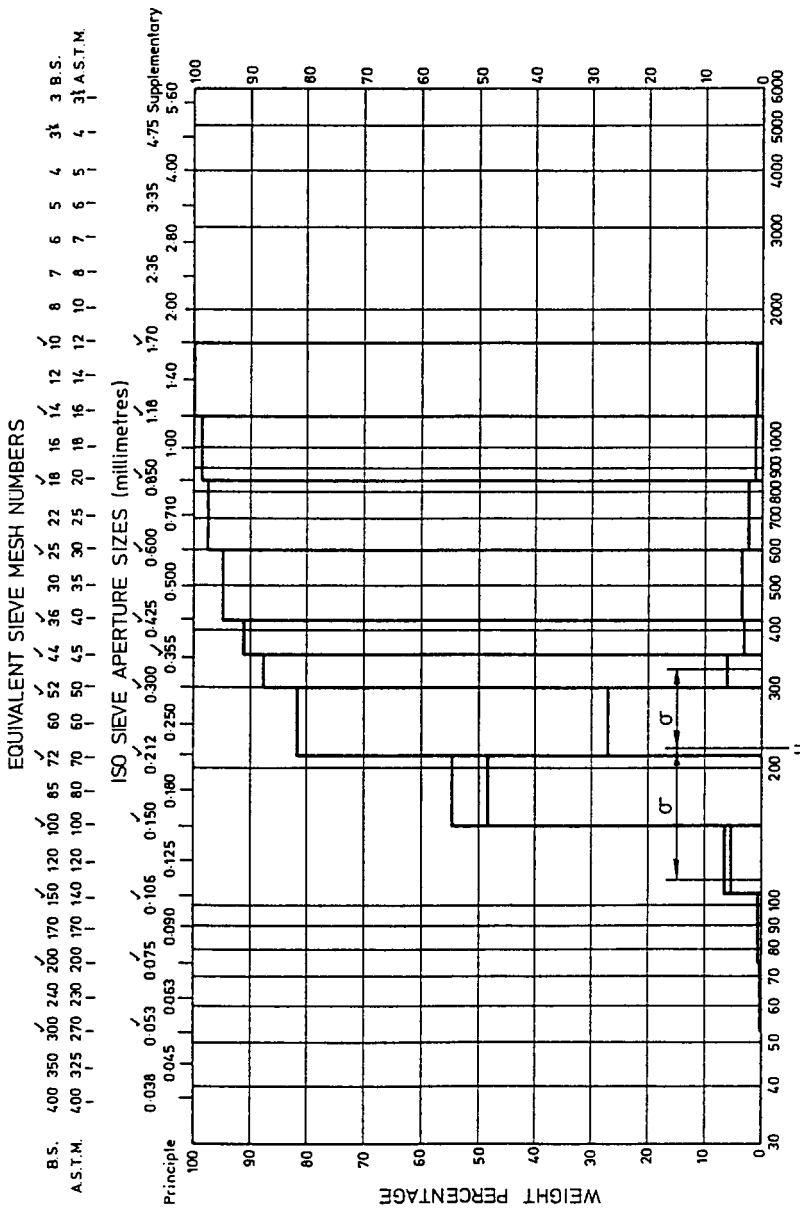

MESH No.	APERTURE SIZE micron	WEIGHT PERCENTAGES Fractional	WEIGHT PERCENTAGES Cumulative
RECEIVER	< 53	——	——
300	53	0.024	0.024
200	75	0.794	0.818
150	106	5.755	6.573
100	150	48.129	54.702
72	212	26.980	81.682
52	300	6.066	87.748
44	355	3.329	91.077
36	425	3.732	94.809
25	600	2.571	97.380
18	850	1.338	98.718
14	1180	1.281	99.999
10	1700	——	——

REMARKS: Material 'Victan' Polyvinylidene Chloride Copolymer Resin VR562.
Note that the sieved distribution has had both its tails truncated by omitting particles <53 μm and >1700 μm.

Fig. 2. Sieve analysis histogram for PVdC powder.

Table 2. Details of the six synthesized distributions

Distribution No.	No. of sieved intervals	Distribution consists of interval No.(s)	Mean particle size μ	3rd moment of μ_3 $E(\mu)$	SD σ	Ratio $v = \sigma/\mu$
1	2	1–2	89.41	721599.02	5.25	0.059
56	1	5	256.00	17148900	22.00	0.086
8	2	8–9	581.64	214806465	99.56	0.171
46	8	1–8	213.96	13811771.4	72.99	0.341
40	6	6–11	411.86	127973824	176.58	0.429
55	11	1–11	221.98	24443068	107.05	0.482

column 12 in Table 1. It was then necessary to find the relationship between the mean number of particles per UV and the ratio σ/μ. This was achieved by *synthesizing* the individually sieved intervals in different combinations to form new particle size distributions which had different ratios of σ/μ. These ratios were then plotted against the mean number of particles per UV. The criterion for forming these new distributions was that a distribution could vary from one having a minimum of two adjacent intervals up to the complete continuous distribution with eleven intervals, i.e. the complete distribution could have its tails at either or both ends truncated to varying degrees. The number of possible unique combinations of continuous distributions was 55 including the complete continuous distribution.

As expected, the largest ratio of σ/μ was for the complete continuous distribution having 11 intervals which was labelled distribution number 55. It was decided to chose four other ratios from the remaining 54 distributions in such a way as to space them as evenly as possible between the largest value and the smallest value. As an additional point, use was made of the single interval number 5, which contained the mean particle size from the complete continuous distribution. This single interval was labelled distribution number 56. Table 2 shows details of the six synthesized distributions used to obtain different ratios of σ/μ. They are listed in order of increasing ratio.

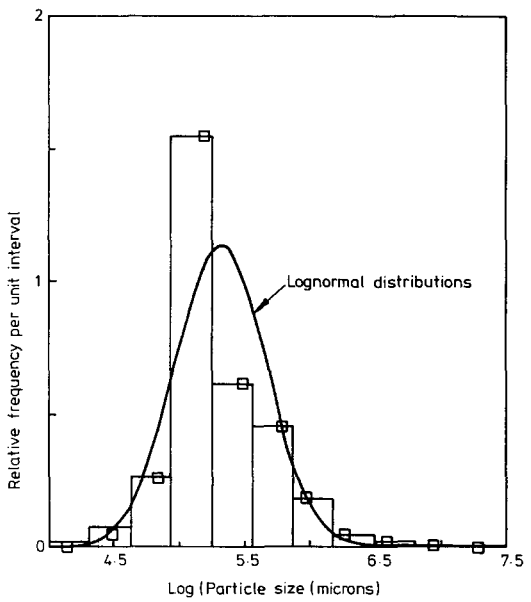

Fig. 3. Histogram of relative frequency per unit interval.

To find the mean number of particles per UV for the six distributions selected, two experiments were designed to study two reproducible states of random packing. They were

(1) the *loose random packing* (LRP) of the particles into a UV
(2) the *dense random packing* (DRP) of the particles into a UV, with vibration.

LRP of particles

The first series of experiments involved LRP of powder particles into a graduated Pyrex cylinder with an i.d. of approx. 24 mm. The cylinder was modified to hold a UV of 40 cm^3. In order to ensure that the required volume was properly filled, a Perspex extension cylinder was manufactured to locate on the o.d. and also to extend the height of the i.d. of the graduated cylinder. The procedure used for filling the cylinder was as follows. Care was taken to ensure that the inside of the cylinder with extension tube was clean and free from moisture. The graduated cylinder by itself was placed on to an electronic digital top pan balance (Sartorius 1212 MP) set for the measuring range 0–300 g. The weight was tared off until it read zero. The graduated cylinder was then placed into a specially designed wooden rig and clamped rigidly into position. The extension cylinder was next pushed over the graduated cylinder until it was firmly located. By using a plastic funnel, the cylinder was gently filled with a pre-weighed 14 g of powder. This amount ensured that it filled the volume above the 40 cm^3 level and in addition by maintaining constant weight ensured that each fill was performed under the same conditions. Figure 4 shows a photograph of the rig with the cylinder immediately after filling. The extension cylinder was then carefully slid off the cylinder, and the excess powder mound levelled by using the edge of a rule (Fig. 5). The powder dust clinging to the outside surface of the cylinder was removed with the aid of a paint brush before placing it back on to the top pan balance. The precise amount of powder in the cylinder was then noted. The powder was emptied from the cylinder and the cylinder and rig were thoroughly cleaned before repeating another test. Each of the six synthesized distributions of powder was sampled in this way to obtain 10 observations of the random variable, W, of the weight of particles per UV.

DRP of particles

The second series of experiments involved the DRP of particles into the graduated cylinder. The increase

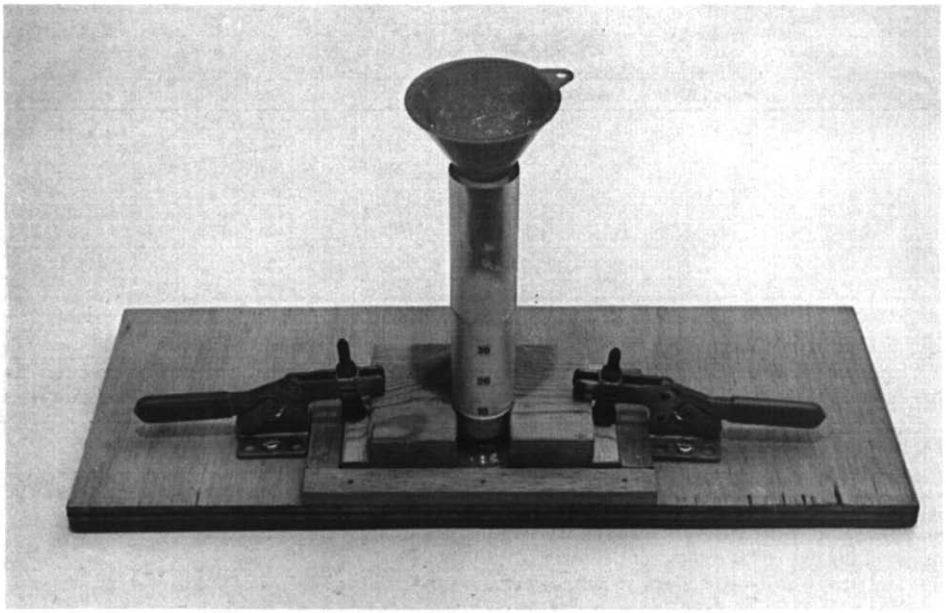

Fig. 4. LRP of particles immediately after depositing powder.

in the packing density of the particles was obtained by increasing the weight of the particles per *UV* using vibratory energy. This was achieved by using an electro-magnetically operated vibratory trough feeder [Valley Products (Lye) Limited, Model MIL]. The graduated cylinder was bolted rigidly to the feed trough using a wooden plate. The extension cylinder was used as before. Because the volume of particles decreased with vibration, the pre-weighed amount of particles was increased to 16 g. The vibrator was switched on with the intensity of vibration set at 20% of full range. In order to ascertain the parameters of vibration at this setting, a Vibration Analyser (Mech-analysis Limited, Model No. IRD 350M) was used. The probe from this instrument was held vertically onto the surface of the trough feeder underneath where the cylinder was located, to obtain the following three parameters of vibration:

(i) frequency, 100 cycles/sec;
(ii) displacement, 0.1 mm peak to peak;
(iii) velocity, 30 mm/sec peak.

Using the first two parameters of frequency and displacement, a fourth parameter of acceleration was then calculated:

(iv) acceleration, (2.1 g) 20.6 m/sec^2 peak.

The plastic funnel was placed into the extension cylinder and the amount of powder was poured into the cylinder. As soon as the powder was deposited, a

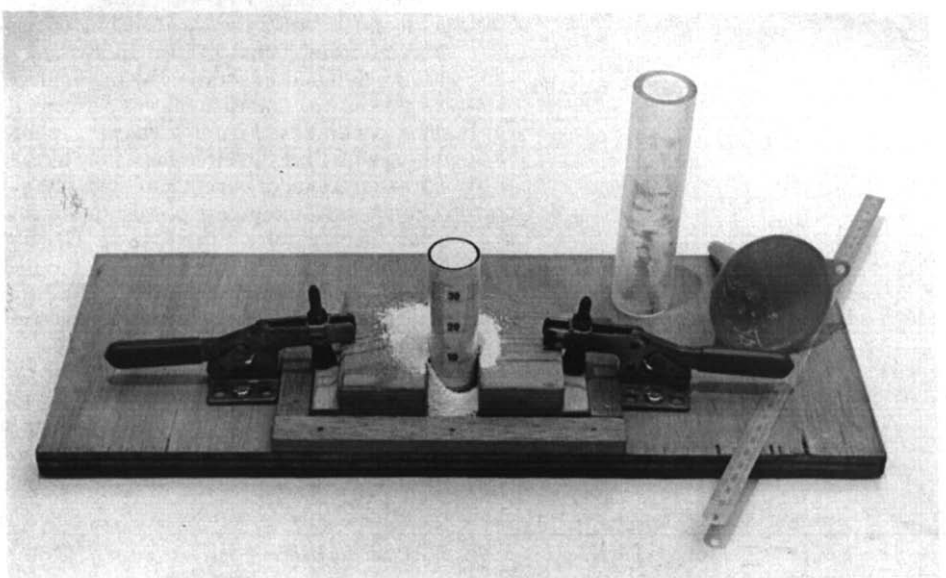

Fig. 5. LRP of particles after levelling of powder.

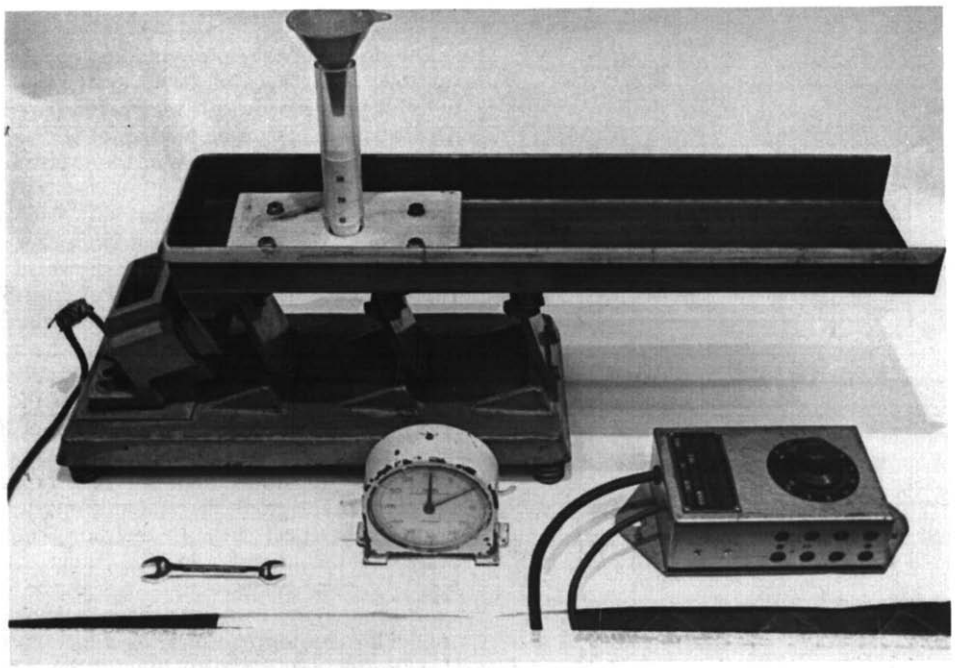

Fig. 6. DRP of particles immediately after depositing powder.

stop clock was started and the funnel was allowed to vibrate for 15 sec (in order for any particles clinging to its surface to fall in) before being removed. Figure 6 shows a photograph of the set-up after the powder was deposited. The vibration was continued for a further 45 sec before being stopped abruptly. The extension cylinder was removed and the powder mound levelled as before. Figure 7 shows a photograph of the set-up after the levelling of the powder. The cylinder was then released from the feed trough and the outside surface was cleaned of any dust particles before being placed on the top pan balance to record the weight of powder. These experiments were repeated to obtain 10 observations of the random variable, W, of the weight of particles per UV for each of the six synthesized distributions.

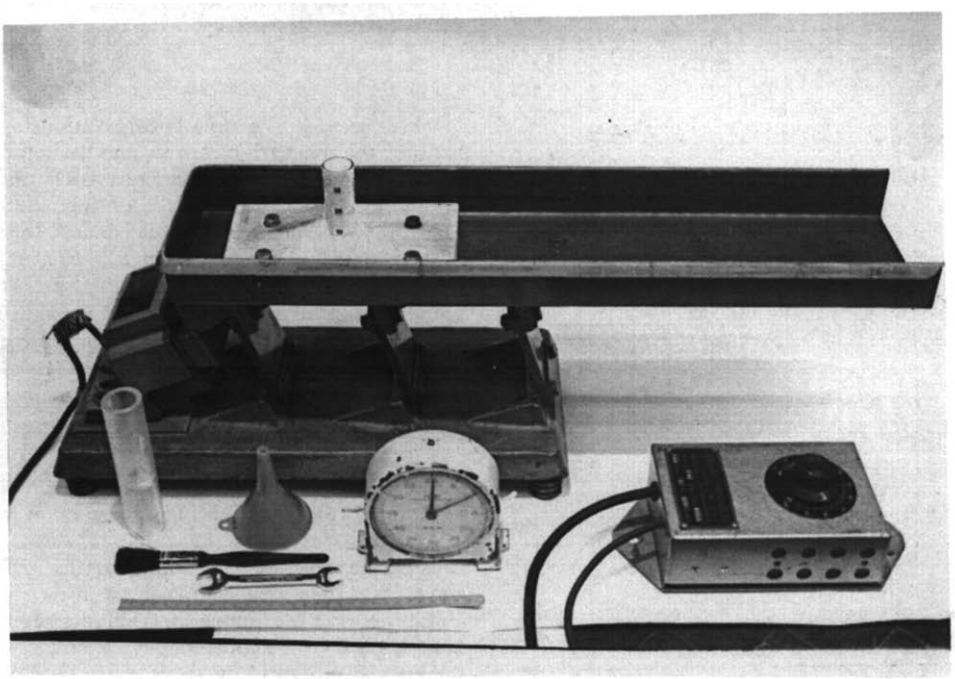

Fig. 7. DRP of particles after vibrating and levelling.

Table 3

Distribution No.	No. of sieved intervals	Distribution consists of inverval No.(s)	State of random packing	Mean number of particles per *UV* for 10 observations										Sample mean of *FTD*	Sample SD of *FTD*
				1	2	3	4	5	6	7	8	9	10		
55	11	1–11	LRP	0.164	0.165	0.166	0.168	0.165	0.166	0.165	0.168	0.170	0.163	0.166	0.00200
55	11	1–11	DRP	0.202	0.202	0.203	0.204	0.203	0.203	0.203	0.201	0.201	0.201	0.202	0.00096

Table 4. Results for the complete continuous distribution

Distribution No.	No. of sieved intervals	Distribution consists of interval No.(s)	State of random packing	*FTD*										Sample mean of μ_N	Sample SD of μ_N
				1	2	3	4	5	6	7	8	9	10		
55	11	1–11	LRP	511,379	515,514	517,811	523,784	515,514	517,811	514,595	523,325	530,217	509,541	517,949	6240
55	11	1–11	DRP	631,758	630,839	634,974	635,893	635,433	634,055	633,595	628,541	627,622	629,460	632,217	3001

CALCULATION OF RESULTS

The results of the 10 observations of the random variable; W, for each of the six synthesized distributions for both experiments were used in equation (14) to calculate, f_N, the mean number of particles per UV for each observation. The value of the absolute solids density, ρ_a, for the grade of PVdC used is 1.7 g/cc—this value was obtained from ICI. The values of $E(\mu^3)$ for all the synthesized distributions were calculated using a computer and are shown in Table 2. Table 3 shows the results for LRP and DRP performed on the complete continuous distribution. This table also shows the sample mean and the sample SD of the 10 observations of the mean number of particles per UV. Figure 8 shows a graph of the six ratio of σ/μ plotted against the sample mean of the mean number of particles per UV . The scatter band for each of the 10 observations for each experiment is also shown. The graph shows that it was not possible to fit a theoretical curve to the data, due to there being a discontinuity in the range $0.059 \leqslant \sigma/\mu \leqslant 0.086$. The relationship can only be described approximately by a *step function* as shown on the graph. In addition to using this function, equation (17) also requires the calculation of the 3rd moment of μ, $[E(\mu^3)]$ which is needed for each particle size distribution. It can be seen by referring to Table 1 that these calculations are quite tedious, so it was decided to eliminate these two functions from equation (17). To find an alternative relationship, it was necessary to plot the ratios of σ/μ directly against the sample means of the *FTD* for both states of packing.

Table 4 shows the results of the calculated *FTD* for the two states of packing for distribution number 55. This table also shows the sample mean and sample SD of the 10 observations of the *FTD*. Figure 9 shows a graph of the six ratios σ/μ plotted against the sample mean of the *FTD*. A 95% confidence interval $(\pm 2\sigma)$ for each of the 10 observations for each state of packing is also shown.

Curve fitting

It was decided to see if a linear relationship existed between the two variables, σ/μ, and the sample mean of the *FTD* in Fig. 9 for both LRP and DRP. Therefore, it was necessary to consider the problem of fitting two straight and parallel lines to the six pairs of data $[(\sigma/\mu)_1, FTD_1,], \ldots, [(\sigma/\mu)_6, FTD_6]$, for each state of packing, where FTD_is values are subject to scatter but those of $(\sigma/\mu)_i$s are not. Straight lines for the LRP and DRP respectively were represented by the equations:

$$FTD_{\text{LRP}} = a_0 + a_1(\sigma/\mu) \tag{18}$$

$$FTD_{\text{DRP}} = a_0 + a_s + a_1(\sigma/\mu). \tag{19}$$

In order to keep the lines parallel, it was first necessary to estimate the slope of the curve, a_1, considering both sets of data together. This parameter was then used with each set of data individually to obtain the estimate for each intercept. To find the estimates of the constants, a_0, a_s and a_1 such that the lines give a good fit to the data, the "*method of least squares*" was used. The estimates, $\hat{a}_0$, $\hat{a}_1$ and $\hat{a}_s$

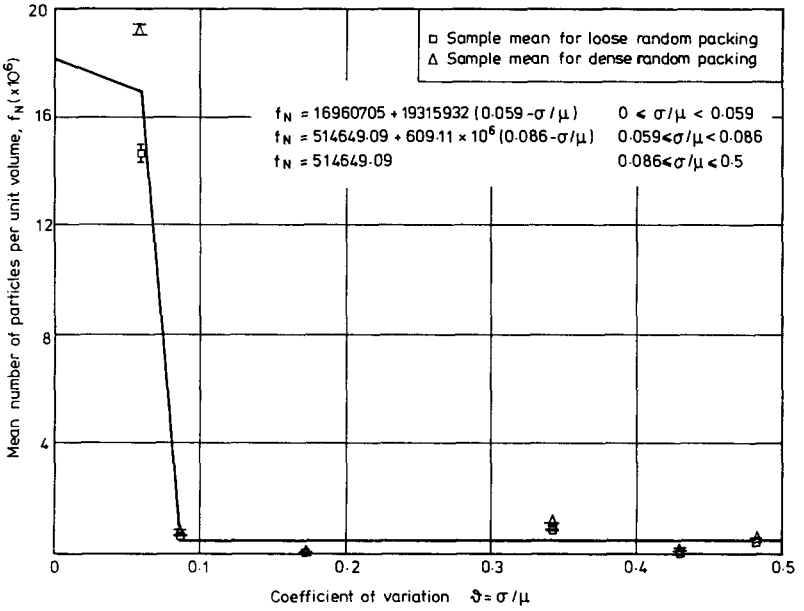

Fig. 8. Variation of the mean number of particles per *UV* with the coefficient of variation.

were obtained as:

$$\hat{a}_0 = 0.14895$$

$$\hat{a}_1 = 0.028908$$

and

$$\hat{a}_2 = 0.035167.$$

These estimates were determined by using the sample mean of the 10 observations of the, *FTD*, corresponding to the six ratios, σ/μ, for both states of packing. Thus the estimated regression line of *FTD* on σ/μ for LRP is given by:

$$FTD_{\text{LRP}} = 0.14895 + 0.028908\,(\sigma/\mu) \qquad (20)$$

and for DRP:

$$FTD_{\text{DRP}} = 0.184117 + 0.028908\,(\sigma/\mu). \qquad (21)$$

Both these lines are shown in Fig. 9.

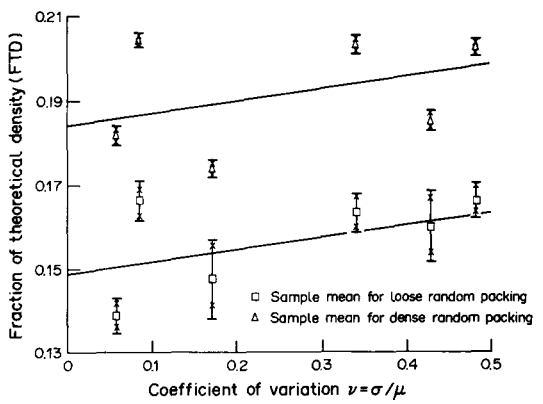

Fig. 9. Variation of the *FTD* with the coefficient of variation.

Examination of residuals

In order to check the assumptions on which the above models were based, it was necessary to look at the *residuals*. A residual is the difference between an observation and the value predicted after fitting the model.

$$\text{Residual} = \text{observation} - \text{fitted value}. \qquad (22)$$

Figure 10 shows a graph of the sample means of the values of *FTD*, plotted vs the residuals. A 95% confidence interval is shown also. A preliminary examination of these residuals was sufficient to detect any gross errors in the proposed models. In this case, it can be seen that the residuals appear non-random

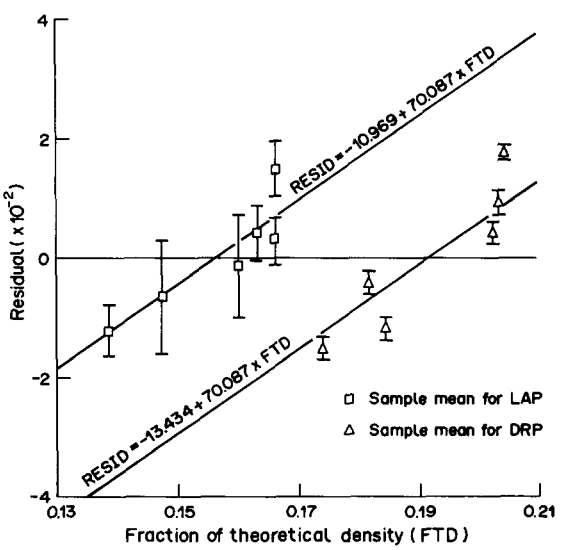

Fig. 10. Residuals as a function of *FTD*.

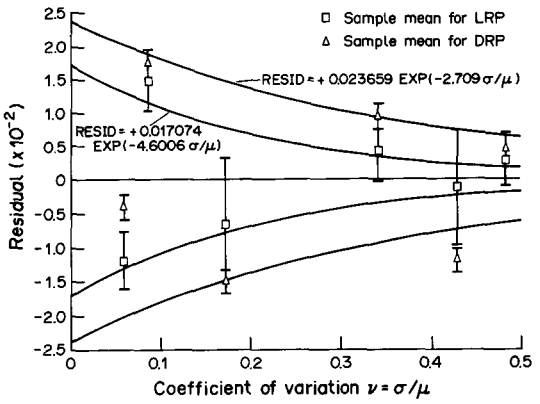

Fig. 11. Variation of the *FTD* with the density of variation.

and are close to the least squares lines, and so it can be seen that each set of data has structure. In other words, the linear models describe the general trend well but they are not a good fit to the data. Thus the structure in the residuals cannot be ignored and needs to be taken into account.

To achieve this, a plot of the residuals against the variable σ/μ was used (see Fig. 11). A 95% confidence interval is shown here also. An exponential relationship was fitted to both sets of data using the method of least squares. This relationship has the form:

$$\text{RESID}_{\text{LRP}} = \pm R_1 \exp[-c_1(\sigma/\mu)] \quad (23)$$

$$\text{RESID}_{\text{DRP}} = \pm R_2 \exp[-c_2(\sigma/\mu)] \quad (24)$$

where R and c are constants.

The constants R_1 and c_1 for LRP were found by assuming all the values were of the same sign, yielding:

$$R_1 = 0.017074$$

$$c_1 = -4.6006.$$

The constants R_2 and c_2 for DRP were found in a similar manner except that the first data point was not used in the calculation as it was considered as an outlier.

$$R_2 = 0.023659$$

$$c_2 = -2.709.$$

The estimated regression line of the residuals on σ/μ for LRP is given by:

$$\text{RESID}_{\text{LRP}} = \pm 0.017074 \exp(-4.6006\,\sigma/\mu) \quad (25)$$

and for DRP:

$$\text{RESID}_{\text{DRP}} = \pm 0.023659 \exp(-2.709\,\sigma/\mu). \quad (26)$$

Hence the complete model for LRP is given by:

$$FTD_{\text{LRP}} = 0.14895 + 0.028908\,(\sigma/\mu) \pm 0.01707 \exp(-4.6006\,\sigma/\mu) \quad (27)$$

and for DRP:

$$FTD_{\text{DRP}} = 0.184117 + 0.028908\,(\sigma/\mu) \pm 0.023659 \exp(-2.709\,\sigma/\mu). \quad (28)$$

The residual lines are shown plotted in Fig. 11.

DISCUSSION AND CONCLUSIONS

It can be seen from Fig. 9 that as the ratio σ/μ decreases so does the *FTD* for both LRP and DRP. The reason for this is that ratios of σ/μ close to zero are associated with small values of μ and very small values of σ. Hence, it is apparent that, as the particle size decreases, friction, adhesion and other surface forces become increasingly important since the surface area to volume ratio of the material increases markedly. These factors can be expected to contribute to bridging and arching in the particle system and consequently to produce increasing levels of porosity with decreasing particle size. The use of vibratory energy to achieve DRP increased *FTD* by 0.035 over the value obtained for LRP.

It can be concluded from these results that, when packing real powder particles, the resultant packing density is extremely low. For example if a powder has a ratio σ/μ of 0.482 (the ratio calculated for the PVdC powder), substitution of this value into equations (20) and (21) yields respectively the *FTD* for LRP of 0.163 and the *FTD* for DRP of 0.198 (note, that these values ignore the effect of the residuals). Both these values can be compared with the values obtained by Scott [3]. His values for the idealized random packing of mono-size spheres in a cylinder of infinite height and infinite dia were 0.601 for LRP and 0.637 for DRP. It is clear that his values for the random packing density of mono-size spheres in space are 3 times greater than the values obtained for packing real powder particles. This is a large differencc and is due to the irregular shape of the real particles and the other factors mentioned above.

REFERENCES

1. D. J. Cumberland and R. J. Crawford. The Packing of Particles. In *Handbook of Powder Technology*, Vol. 6. Elsevier, Amsterdam (1987).
2. E. Kreyszig. *Introductory Mathematical Statistics*, pp. 254–257, 453. Wiley, New York (1970).
3. G. D. Scott. *Nature* **188**, 908–909 (1960).